

**Inter-annual surface  
evolution of an  
Antarctic blue-ice  
moraine**

M. J. Westoby et al.

This discussion paper is/has been under review for the journal Earth Surface Dynamics (ESurfD).  
Please refer to the corresponding final paper in ESurf if available.

# Inter-annual surface evolution of an Antarctic blue-ice moraine using multi-temporal DEMs

**M. J. Westoby<sup>1</sup>, S. A. Dunning<sup>2</sup>, J. Woodward<sup>1</sup>, A. S. Hein<sup>3</sup>, S. M. Marrero<sup>3</sup>,  
K. Winter<sup>1</sup>, and D. E. Sugden<sup>3</sup>**

<sup>1</sup>Department of Geography, Engineering and Environment, Northumbria University,  
Newcastle upon Tyne, UK

<sup>2</sup>School of Geography, Politics and Sociology, Newcastle University, Newcastle upon Tyne, UK

<sup>3</sup>School of GeoSciences, University of Edinburgh, Edinburgh, UK

Received: 29 October 2015 – Accepted: 3 November 2015 – Published: 18 November 2015

Correspondence to: M. J. Westoby (matt.westoby@northumbria.ac.uk)

Published by Copernicus Publications on behalf of the European Geosciences Union.

Title Page

Abstract

Introduction

Conclusions

References

Tables

Figures



Back

Close

Full Screen / Esc

Printer-friendly Version

Interactive Discussion



## Abstract

Multi-temporal and fine resolution topographic data products are being increasingly used to quantify surface elevation change in glacial environments. In this study, we employ 3-D digital elevation model (DEM) differencing to quantify the topographic evolution of a blue-ice moraine complex in front of Patriot Hills, Heritage Range, Antarctica. Terrestrial laser scanning (TLS) was used to acquire multiple topographic datasets of the moraine surface at the beginning and end of the austral summer season in 2012/2013 and during a resurvey field campaign in 2014. A complementary topographic dataset was acquired at the end of season 1 through the application of Structure-from-Motion (SfM) photogrammetry to a set of aerial photographs taken from an unmanned aerial vehicle (UAV). Three-dimensional cloud-to-cloud differencing was undertaken using the Multiscale Model to Model Cloud Comparison (M3C2) algorithm. DEM differencing revealed net uplift and lateral movement of the moraine crests within season 1 (mean uplift  $\sim 0.10$  m), with lowering of a similar magnitude in some inter-moraine depressions and close to the current ice margin. Our results indicate net uplift across the site between seasons 1 and 2 (mean  $0.07$  m). This research demonstrates that it is possible to detect dynamic surface topographical change across glacial moraines over short (annual to intra-annual) timescales through the acquisition and differencing of fine-resolution topographic datasets. Such data offer new opportunities to understand the process linkages between surface ablation, ice flow, and debris supply within moraine ice.

## 1 Introduction

Fine-resolution topographic data products are now routinely used for the geomorphometric characterisation of Earth surface landforms (e.g. Passalacqua et al., 2014, 2015; Tarolli, 2014). Recent decades have seen the advent and uptake of a range of surveying technologies for characterising the form and evolution of Earth surface topography

**ESURFD**

3, 1317–1344, 2015

### Inter-annual surface evolution of an Antarctic blue-ice moraine

M. J. Westoby et al.

Title Page

Abstract

Introduction

Conclusions

References

Tables

Figures



Back

Close

Full Screen / Esc

Printer-friendly Version

Interactive Discussion









## 3.1 Topographic data acquisition

### 3.1.1 Terrestrial laser scanning

TLS data were acquired using a Riegl LMS-Z620 time-of-flight laser scanner, set to acquire  $\sim 11\,000$  points  $s^{-1}$  in the near-infrared band at horizontal and vertical scanning increments of  $0.031^\circ$ , equivalent to a point spacing of 0.05 m at a distance of 100 m and with a beam divergence of 15 mm per 100 m. Data were acquired from six locations across the site at the beginning of season 1 (7–11 December 2012; Fig. 1; Table 1). Two of these positions were re-occupied at the end of season 1 (9 January 2013) and three positions were reoccupied in season 2 (Fig. 1; 14 January 2014). Following manual editing and the automated removal of isolated points to improve data quality, each set of scans were co-registered in Riegl RiSCAN PRO software (v. 1.5.9) using a two-step procedure employing coarse manual point-matching followed by the application of a linear, iterative, least-squares minimisation solution to reduce residual alignment error. Individual scans were then merged to produce a single 3-D point cloud for each scan date. Merged scan data from the end of seasons 1 and 2 were subsequently registered to the scan data from the beginning of season 1 using the methods described above (Table 1).

### 3.1.2 Structure-from-Motion with Multi-View Stereo photogrammetry

Low-altitude aerial photographs of the study site were acquired using a 10-Megapixel Panasonic Lumix DMC-LX5 compact digital camera with a fixed focal length (8 mm) and automatic exposure settings, mounted in a fixed, downward-facing (nadir) perspective on a sub-5 kg fixed-wing UAV. Photographs were acquired in a single sortie lasting  $\sim 5$  min. A total of 155 photographs were acquired at a 2 s interval at an approximate ground height of 120 m, producing an average image overlap of 80 %, and an approximate ground resolution of  $0.07\text{ m}^2$  per pixel. Mean point density was  $\sim 300$  points  $m^{-2}$ , compared to a mean of  $278$  points  $m^{-2}$  for the TLS datasets. Motion blur of the input

## Inter-annual surface evolution of an Antarctic blue-ice moraine

M. J. Westoby et al.

Title Page

Abstract

Introduction

Conclusions

References

Tables

Figures



Back

Close

Full Screen / Esc

Printer-friendly Version

Interactive Discussion



images was negligible due to favourable image exposure conditions and an appropriate UAV flying height and speed.

UAV photographs were used as input to SfM reconstruction using the proprietary Agisoft PhotoScan Professional Edition (v. 1.1.6) software. Unique image tie-points which are stable under variations in view perspective and lighting are identified and matched across input photographs, similar to Lowe's (2004) Scale Invariant Feature Transform (SIFT) method. An iterative bundle adjustment algorithm is used to solve for internal and external camera orientation parameters and produce a sparse 3-D point cloud. The results of the first-pass camera pose estimation were scrutinised and only 3-D points which appear in a minimum of 3 photographs and possessed a reprojection error of  $< 1.0$  were retained. A two-phase method of UAV-SfM data registration was employed: (1) ground control was obtained by identifying common features in the UAV-SfM photographs and TLS data from the end of season 1 (acquired 4 days after the SfM data; Table 1), such as the corners of large, well-resolved boulders. GCP data were used to optimise the initial camera alignment and transform the regenerated UAV-SfM data to the same object space as the TLS data, producing an xyz RMS error of 0.23 m. (2) following dense reconstruction, 3-D point data were exported to RiSCAN PRO (v. 1.5.9) software, and a linear, iterative, least-squares minimisation employing surface plane matching was used to improve the alignment and reduce the xyz RMS error to 0.03 m.

### 3.2 Cloud-to-cloud differencing

Three-dimensional "cloud-to-cloud" distance calculations were used to quantify moraine surface evolution (e.g. Lague et al., 2013). Since the dominant direction of surface evolution across the study site was unknown a priori, the application of an algorithm that is capable of detecting fully three-dimensional topographic change was deemed to be the most appropriate method in this context. To this end, we employ the Multiscale Model to Model Cloud Comparison (M3C2) algorithm (Lague et al., 2013;

# ESURFD

3, 1317–1344, 2015

## Inter-annual surface evolution of an Antarctic blue-ice moraine

M. J. Westoby et al.

Title Page

Abstract

Introduction

Conclusions

References

Tables

Figures



Back

Close

Full Screen / Esc

Printer-friendly Version

Interactive Discussion





masked to exclude points where change is lower than level of detection threshold for a 95 % confidence level,  $LoD_{95\%}(d)$ , which is defined as:

$$LoD_{95\%}(d) = \pm 1.96 \left( \frac{\sigma_1(d)^2}{n_1} + \frac{\sigma_2(d)^2}{n_2} + \text{reg} \right), \quad (2)$$

where  $d$  is the radius of the projection cylinder,  $\text{reg}$  is the user-specified registration error, for which we substitute the propagated root mean square alignment error for point clouds  $n_1$  and  $n_2$  (Table 2; Eq. 1) and assume that this error is isotropic and spatially uniform across the dataset.

To calculate the total propagated error for each differencing epoch,  $\sigma_{DoD}$ , the estimates of errors in each point cloud (i.e. the sum of the average scan-scan RMS error and a project-project RMS error, where applicable) were combined using:

$$\sigma_{DoD} = \sqrt{\sigma_{C_1}^2 + \sigma_{C_2}^2}, \quad (3)$$

where  $\sigma_{C_1}^2$  and  $\sigma_{C_2}^2$  are the RMS errors associated with point clouds  $C_1$  and  $C_2$ .

#### 4 Short-term topographic evolution of blue-ice moraines

The results of 3-D cloud-to-cloud differencing are summarised in Figs. 3 to 5. Threshold levels of change detection ranged from 0.094–0.103 m. The upper (i.e. most conservative) bound of this range was applied to the results from all differencing epochs, so that only 3-D surface changes greater than 0.103 m were considered in the subsequent analysis. The horizontal ( $xy$ ) and vertical ( $z$ ) components of 3-D surface change were separated to aid the analysis and interpretation of moraine surface evolution. Vertical surface changes for a range of epochs, encompassing intra-annual and annual change, are displayed in Fig. 3, whilst the horizontal component of 3-D change are shown in Fig. 4. The longest differencing epoch, representing a period of  $\sim 400$  days (Fig. 3b)

### Inter-annual surface evolution of an Antarctic blue-ice moraine

M. J. Westoby et al.

Title Page

Abstract

Introduction

Conclusions

References

Tables

Figures

◀

▶

◀

▶

Back

Close

Full Screen / Esc

Printer-friendly Version

Interactive Discussion









of additional, oblique imagery, and use of suitable GCPs (James and Robson, 2014). However, although the latter were relatively evenly spaced across our study site, the inclusion of these data and subsequent use for the optimisation of the SfM data prior to dense point cloud reconstruction does not appear to have altogether eliminated these model deformations (Fig. 5).

The above shortcomings notwithstanding, this research nevertheless represents the first successful application of a combination of high resolution surveying methods for quantifying the topographic evolution of ice-marginal topography in this environment. This study has demonstrated that, whilst a number of operational considerations, such as the requirement for multiple TLS station positions to acquire satisfactory spatial coverage across a topographically complex site of this size, and the necessary deployment of an independent set of dedicated GCPs for accurate UAV-SfM georegistration or the acquisition of additional, oblique aerial photographs, must be taken into account, these technologies are appropriate for reconstructing blue-ice moraine surface topography. Furthermore, the use of fully 3-D differencing algorithms is appropriate for quantifying inter-annual to annual moraine surface evolution.

A comprehensive analysis of the evolution of the Patriot Hills blue-ice moraine and its relationships to ablation and underlying ice structure is the focus of another study, but it is worth highlighting some implications arising from the measurement of these short-term changes in surface morphology. Firstly, the moraine ridges both close to, and far from the ice margin emerge as axes of activity and uplift (Fig. 3c). This activity is not simply confined to “inward” or “outward” movement of moraines within the embayment, but also involves a lateral component. Secondly, the surface lowering is the result of ablation and it is notable that most lowering occurred near the ice margin where the debris layer is typically thinnest and less than  $\sim 0.15$  m. Finally, the close match of surface elevation cross-profiles between seasons (Fig. 5) points to medium-term stability of the moraine system. This conclusion will be investigated through the application of cosmogenic isotope evidence to assess change since the Holocene.

**Inter-annual surface evolution of an Antarctic blue-ice moraine**

M. J. Westoby et al.

Title Page

Abstract

Introduction

Conclusions

References

Tables

Figures

◀

▶

◀

▶

Back

Close

Full Screen / Esc

Printer-friendly Version

Interactive Discussion



## 5 Summary

This research has employed a combination of TLS and UAV-based SfM-MVS photogrammetry and 3-D differencing methods to quantify the topographic evolution of an Antarctic blue-ice moraine complex over annual and intra-annual timescales. Segmentation of lateral and vertical surface displacements reveal site- and local-scale patterns of geomorphometric moraine surface evolution beyond a threshold level of detection (95 % confidence), including largely persistent vertical uplift across key moraine ridges, both within a single season, and between seasons. This persistent uplift is interspersed with areas (and periods) of surface downwasting which is largely confined to the rear of the moraine basin for both differencing epochs, and in ice-marginal regions within season 1. Analysis of lateral displacement vectors, which are generally of a much smaller magnitude than vertical displacements, provide further insights into moraine surface evolution. A number of methodological shortcomings are highlighted. Briefly, these relate to the incomplete spatial coverage afforded by the use of TLS in a topographically complex environment, and issues associated with obtaining suitable ground control for SfM-MVS processing and potential implications for the accuracy of SfM-derived topographic data products. The research represents the first successful application of these techniques in such a remote environment.

*Author contributions.* S. A. Dunning, J. Woodward, A. Hein, K. Winter, S. M. Marrero and D. E. Sugden collected field data. TLS and SfM data processing and differencing were undertaken by M. J. Westoby. Data analysis was performed by M. J. Westoby, S. A. Dunning and J. Woodward. Manuscript figures were produced by M. J. Westoby. All authors contributed to the writing and revision of the manuscript.

*Acknowledgements.* The research was funded by the UK Natural Environment Research Council (Research Grants NE/I027576/1, NE/I025840/1, NE/I024194/1, NE/I025263/1). We thank the British Antarctic Survey for logistical support.

# ESURFD

3, 1317–1344, 2015

## Inter-annual surface evolution of an Antarctic blue-ice moraine

M. J. Westoby et al.

Title Page

Abstract

Introduction

Conclusions

References

Tables

Figures



Back

Close

Full Screen / Esc

Printer-friendly Version

Interactive Discussion



## References

- Agisoft: Agisoft PhotoScan Professional Edition v.1.1.6., available at: <http://www.agisoft.com> (last access: 10 September 2015), 2014.
- Arnold, N. S., Rees, W. G., Hodson, A. J., and Kohler, J.: Topographic controls on the surface energy balance of a high Arctic valley glacier, *J. Geophys. Res.*, 111, F02011, doi:10.1029/2005JF000426, 2006.
- Baltsavias, E. P., Favey, E., Bauder, A., Böschi, H., and Pateraki, M.: Digital surface modelling by airborne laser scanning and digital photogrammetry for glacier monitoring, *Photogramm. Rec.*, 17, 243–273, doi:10.1111/0031-868X.00182, 2001.
- Barnhart, T. B. and Crosby, B. T.: Comparing two methods of surface change detection on an evolving thermokarst using high-temporal-frequency terrestrial laser scanning, Selawik River, Alaska, *Remote Sens. Environ.*, 5, 2813–2837, doi:10.3390/rs5062813, 2013.
- Bintanja, R.: On the glaciological, meteorological, and climatological significance of Antarctic blue ice areas, *Rev. Geophys.*, 37, 337–359, doi:10.1029/1999RG900007, 1999.
- Bollmann, E., Sailer, R., Briese, C., Stotter, J., and Fritzmann, P.: Potential of airborne laser scanning for geomorphologic feature and process detection and quantifications in high alpine mountains, *Z. Geomorphol.*, 55, 83–104, doi:10.1127/0372-8854/2011/0055S2-0047, 2011.
- Brasington, J., Rumsby, B. T., and McVey, R. A.: Monitoring and modelling morphological change in a braided gravel-bed river using high resolution GPS-based survey, *Earth Surf. Proc. Land.*, 25, 973–990, doi:10.1002/1096-9837(200008)25:9<973::AID-ESP111>3.0.CO;2-Y, 2000.
- Chandler, B. M. P., Evans, D. J. A., Roberts, D. H., Ewertowski, M., and Clayton, A. I.: Glacial geomorphology of the Skálafellsjökull foreland, Iceland: a case study of “annual” moraines, *J. Maps*, 13 pp., doi:10.1080/17445647.2015.1096216, accepted, 2015.
- Dunning, S. A., Large, A. R. G., Russell, A. J., Roberts, M. J., Duller, R., Woodward, J., Mériaux, A.-S., Tweed, F. S., and Lim, M.: The role of multiple glacier outburst floods in proglacial landscape evolution: the 2010 Eyjafjallajökull eruption, Iceland, *Geology*, 41, 1123–1136, doi:10.1130/G34665.1, 2013.
- Farr, T. G., Rosen, P. A., Caro, E., Crippen, R., Duren, R., Hensley, S., Kobrick, M., Paller, M., Rodriguez, E., Roth, L., Seal, D., Shaffer, S., Shimada, J., Umland, J., Werner, M., Oskin, M., Burbank, D., and Alsdorf, D.: The shuttle radar topography mission, *Rev. Geophys.*, 45, RG2004, doi:10.1029/2005RG000183, 2007.

## Inter-annual surface evolution of an Antarctic blue-ice moraine

M. J. Westoby et al.

Title Page

Abstract

Introduction

Conclusions

References

Tables

Figures



Back

Close

Full Screen / Esc

Printer-friendly Version

Interactive Discussion



## Inter-annual surface evolution of an Antarctic blue-ice moraine

M. J. Westoby et al.

Title Page

Abstract

Introduction

Conclusions

References

Tables

Figures

◀

▶

◀

▶

Back

Close

Full Screen / Esc

Printer-friendly Version

Interactive Discussion



- Fogwill, C. J., Hein, A. S., Bentley, M. J., and Sugden, D. E.: Do blue-ice moraines in the Heritage Range show the West Antarctic ice sheet survived the last interglacial?, *Palaeogeogr. Palaeoclimatol.*, 335–336, 61–70, doi:10.1016/j.palaeo.2011.01.027, 2012.
- Fuller, I. C., Large, A. R. G., and Milan, D.: Quantifying channel development and sediment transfer following chute cutoff in a wandering gravel-bed river, *Geomorphology*, 54, 307–323, doi:10.1016/S0169-555X(02)00374-4, 2003.
- Gabbud, C., Micheletti, N., and Lane, S. N.: Lidar measurement of surface melt for a temperate Alpine glacier at the seasonal and hourly scales, *J. Glaciol.*, 61, 963–974, doi:10.3189/2015JoG14J226, 2015.
- Hardt, J., Hebenstreit, R., Lüthgens, C., and Böse, M.: High-resolution mapping of ice-marginal landforms in the Barnim region, northeast Germany, *Geomorphology*, 250, 41–52, doi:10.1016/j.geomorph.2015.07.045, 2015.
- Hodge, R., Brasington, J., and Richards, K.: In-situ characterisation of grain-scale fluvial morphology using Terrestrial Laser Scanning, *Earth Surf. Proc. Land.*, 34, 954–968, doi:10.1002/esp.1780, 2009.
- Immerzeel, W. W., Kraaijenbrink, P. D. A., Shea, J. M., Shrestha, A. B., Pellicciotti, F., Bierkens, M. F. P., and de Jong, S. M.: High-resolution monitoring of Himalayan glacier dynamics using unmanned aerial vehicles, *Remote Sens. Environ.*, 150, 93–103, doi:10.1016/j.rse.2014.04.025, 2014.
- Irvine-Fynn, T. D. L., Sanz-Ablanedo, E., Rutter, N., Smith, M. W., and Chandler, J. H.: Measuring glacier surface roughness using plot-scale, close-range digital photogrammetry, *J. Glaciol.*, 60, 957–969, doi:10.3189/2014JoG14J032, 2014.
- James, M. R. and Robson, S.: Straightforward reconstruction of 3-D surfaces and topography with a camera: accuracy and geoscience application, *J. Geophys. Res.*, 117, F03017, doi:10.1029/2011JF002289, 2012.
- James, M. R. and Robson, S.: Mitigating systematic error in topographic models derived from UAV and ground-based image networks, *Earth Surf. Proc. Land.*, 39, 1413–1420, doi:10.1002/esp.3609, 2014.
- James, M. R., Robson, S., Pinkerton, H., and Ball, M.: Oblique photogrammetry with visible and thermal images of active lava flows, *B. Volcanol.*, 69, 105–108, doi:10.1007/s00445-006-0062-9, 2006.



## Inter-annual surface evolution of an Antarctic blue-ice moraine

M. J. Westoby et al.

Title Page

Abstract

Introduction

Conclusions

References

Tables

Figures



Back

Close

Full Screen / Esc

Printer-friendly Version

Interactive Discussion



Micheletti, N., Lane, S. N., and Chandler, J. H.: Application of archival aerial photogrammetry to quantify climate forcing of Alpine landscapes, *The Photogramm. Rec.*, 30, 143–165, doi:10.1111/phor.12099, 2015.

Milan, D. J., Heritage, G. L., and Hetherington, D.: Application of a 3-D laser scanner in the assessment of erosion and deposition volumes and channel change in a proglacial river, *Earth Surf. Proc. Land.*, 32, 1657–1674, doi:10.1002/esp.1592, 2007.

Niethammer, U., Rothmund, S., James, M. R., Traveletti, J., and Joswig, M.: UAV-based remote sensing of landslide, *International Archives of the Photogrammetry, Remote Sensing and Spatial Information Sciences*, 38, 496–501, doi:10.1016/j.enggeo.2011.03.012, 2010.

Noh, M.-J. and Howat, I. M.: Automated stereo-photogrammetric DEM generation at high latitudes: Surface Extraction with TIN-based Search-space Minimization (SETSM) validation and demonstration over glaciated regions, *Gisci Remote Sens*, 52, 198–217, doi:10.1080/15481603.2015.1008621, 2015.

Ouédraogo, M. M., Degré, A., Debouche, C., and Lisein, J.: The evaluation of unmanned aerial system-based photogrammetry and terrestrial laser scanning to generate DEMs of agricultural watersheds, *Geomorphology*, 214, 339–355, doi:10.1016/j.geomorph.2014.02.016, 2014.

Passalacqua, P., Hillier, J., and Tarolli, P.: Innovative analysis and use of high-resolution DTMs for quantitative interrogation of Earth-surface processes, *Earth Surf. Proc. Land.*, 39, 1400–1403, doi:10.1002/esp.3616, 2014.

Passalacqua, P., Belmont, P., Staley, D. M., Simley, J. D., Arrowsmith, J. R., Bode, C. A., Crosby, C., DeLong, S. B., Glenn, N. F., Kelly, S. A., Lague, D., Sangireddy, H., Schaffrath, K., Tarboton, D. G., Waskiewicz, T., and Wheaton, J. M.: Analyzing high resolution topography for advancing the understanding of mass and energy transfer through landscapes: a review, *Earth-Sci. Rev.*, 148, 174–193, doi:10.1016/j.earscirev.2015.05.012, 2015.

Pepin, N. C., Duane, W. J., Schaefer, M., Pike, G., and Hardy, D. R.: Measuring and modeling the retreat of the summit ice fields on Kilimanjaro, East Africa, *Arct. Antarct. Alp. Res.*, 46, 905–917, doi:10.1657/1938-4246-46.4.905, 2014.

Piermattei, L., Carturan, L., and Guarnieri, A.: Use of terrestrial photogrammetry based on structure-from-motion for mass balance estimation of a small glacier in the Italian alps, *Earth Surf. Proc. Land.*, 40, 1791–1802, doi:10.1002/esp.3756, 2015.







## Inter-annual surface evolution of an Antarctic blue-ice moraine

M. J. Westoby et al.

Title Page

Abstract

Introduction

Conclusions

References

Tables

Figures

◀

▶

◀

▶

Back

Close

Full Screen / Esc

Printer-friendly Version

Interactive Discussion



**Table 1.** Terrestrial laser scanning and UAV-SfM survey dates and registration errors. Within each season, individual scans were registered to a single static position to produce a single, merged point cloud (scan-scan registration error). TLS data from the end of season 1 and for season 2 were subsequently registered to TLS data acquired at the start of season 1, producing a project-project registration error. The UAV-SfM data (season 1 end) were registered to TLS data from the end of season 1.

Field survey	Scan position	Scan date	Scan-scan registration error (RMS; m)	Project-project registration error (RMS; m)
Season 1 start (TLS)	1	07 Dec 2012	Static	Static
	2	08 Dec 2012	0.0327	
	3	08 Dec 2012	0.0391	
	5	09 Dec 2012	0.0301	
	6	01 Dec 2012	0.0258	
	7	11 Dec 2012	0.0258	
	Season 1 end (TLS)	1	09 Jan 2013	
2		09 Jan 2013	0.0145	
Season 1 end (UAV-SfM)	–	05 Jan 2013	–	0.0306
Season 2 (TLS)	1	14 Jan 2014	Static	0.0149
	2	14 Jan 2014	0.0205	
	3	14 Jan 2014	0.0255	



## Inter-annual surface evolution of an Antarctic blue-ice moraine

M. J. Westoby et al.

Title Page

Abstract

Introduction

Conclusions

References

Tables

Figures

◀

▶

◀

▶

Back

Close

Full Screen / Esc

Printer-friendly Version

Interactive Discussion

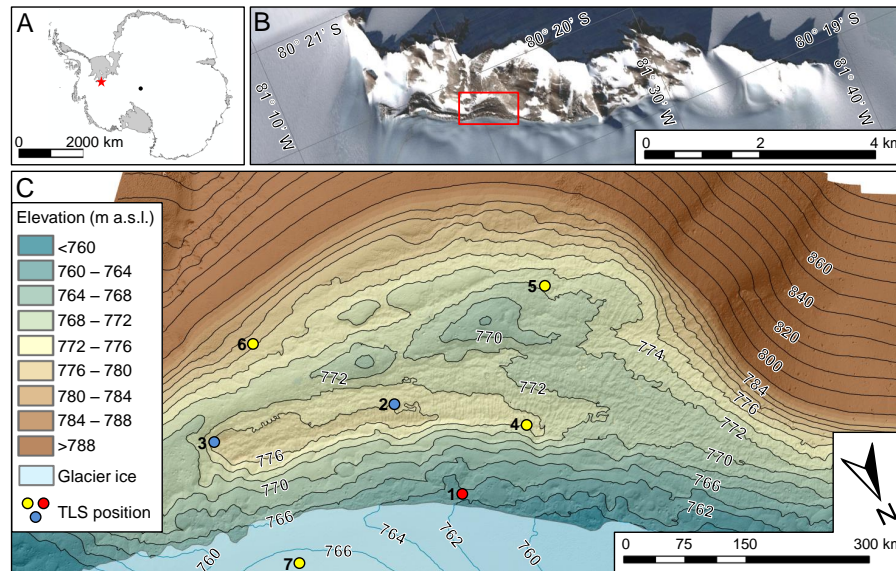


**Figure 1.** Blue-ice moraine embayment, Patriot Hills, Heritage Range, Antarctica. **(a)** Antarctica context map. Red star is location of the Heritage Range. Black dot indicates location of the geographic south pole. **(b)** The Patriot Hills massif. The location of the study embayment and area displayed in **(c)** highlighted in red. **(c)** Detailed study site overview map. Contours and underlying hillshade are derived from a UAV-SfM-derived DEM. TLS scanning positions for the start of season 1 are shown in red, blue and yellow. The two scan positions re-occupied at the end of season 1 are shown in blue, whilst the three scan positions reoccupied in season 2 are shown in blue and red. Background to **(b)** is ©2015 DigitalGlobe, extracted from Google Earth (imagery date: 3 October 2009).

**Inter-annual surface evolution of an Antarctic blue-ice moraine**

M. J. Westoby et al.

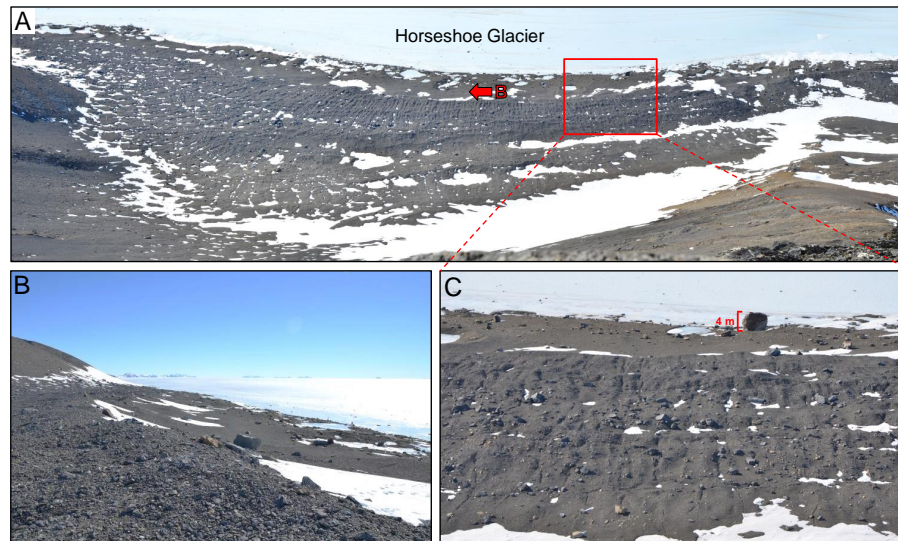


**Figure 2.** Field photographs of the Patriot Hills blue-ice moraine study site. **(a)** Panoramic photograph of the moraine embayment – view north-east towards the ice margin from the rear of the embayment. Area shown in **(c)** and position and view direction of camera **(b)** shown for reference. **(b)** View to the north-west with moraine crest in foreground and subdued, ice-marginal moraine surface topography in middle-ground. **(c)** Close-up of moraine topography, highlighting ridges and furrows on moraine crests and in inter-moraine troughs.

Title Page

Abstract

Introduction

Conclusions

References

Tables

Figures

◀

▶

◀

▶

Back

Close

Full Screen / Esc

Printer-friendly Version

Interactive Discussion



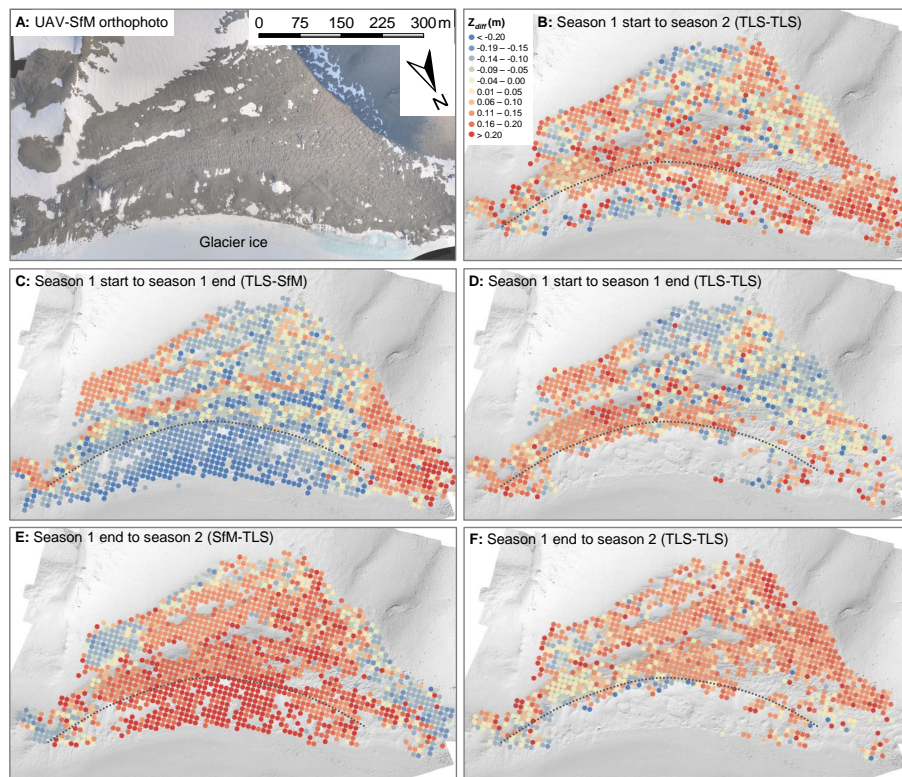


**Figure 3.** Vertical component of 3-D topographic change ( $Z_{diff}$ ) overlain on a UAV-SfM-derived hill-shaded DEM of the Patriot Hills blue-ice moraine complex. Topographic evolution was quantified using the Multiscale Model to Model Cloud Comparison (M3C2) algorithm in CloudCompare software. **(a)** UAV-SfM orthophotograph of the study site. Panels **(b)** to **(f)** cover specific differencing epochs using a combination of TLS and SfM data (see panel headings). Dashed line in **(b)** to **(f)** indicates locations of primary moraine ridge crest.

## Inter-annual surface evolution of an Antarctic blue-ice moraine

M. J. Westoby et al.

Title Page

Abstract

Introduction

Conclusions

References

Tables

Figures

◀

▶

◀

▶

Back

Close

Full Screen / Esc

Printer-friendly Version

Interactive Discussion



## Inter-annual surface evolution of an Antarctic blue-ice moraine

M. J. Westoby et al.

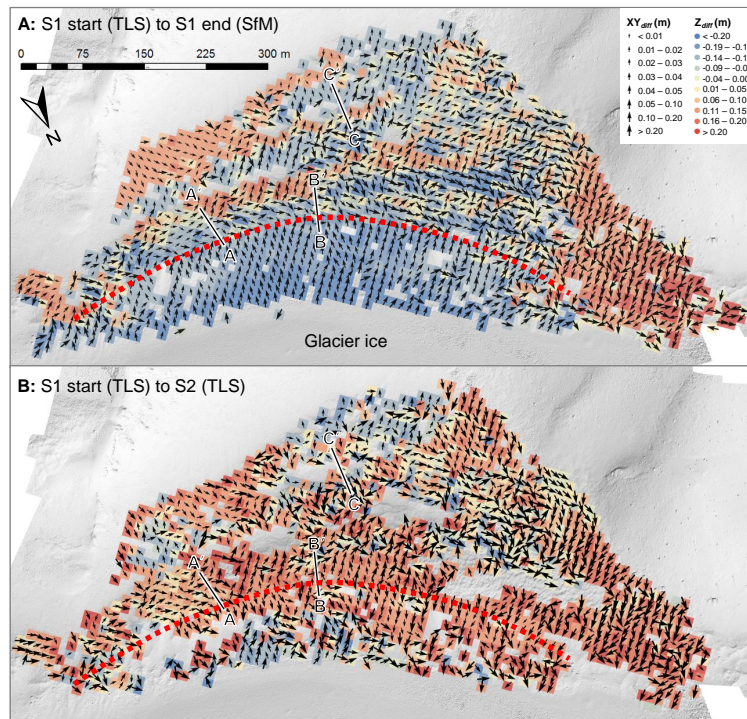


**Figure 4.** Change detection mapping for **(a)** intra-annual (season 1 start to season 1 end) and **(b)** annual (season 1 start to season 2) differencing epochs. Horizontal difference vectors ( $XY_{diff}$ ) are scaled by magnitude and oriented according to the direction of change. The vertical component of 3-D change ( $Z_{diff}$ ) is shown in the background. Transects A–C denote the location of moraine surface profiles displayed in Fig. 5. Red dashes on both panels show approximate location of primary moraine ridge crest.

[Title Page](#)
[Abstract](#)
[Introduction](#)
[Conclusions](#)
[References](#)
[Tables](#)
[Figures](#)
[Back](#)
[Close](#)
[Full Screen / Esc](#)
[Printer-friendly Version](#)
[Interactive Discussion](#)

## Inter-annual surface evolution of an Antarctic blue-ice moraine

M. J. Westoby et al.

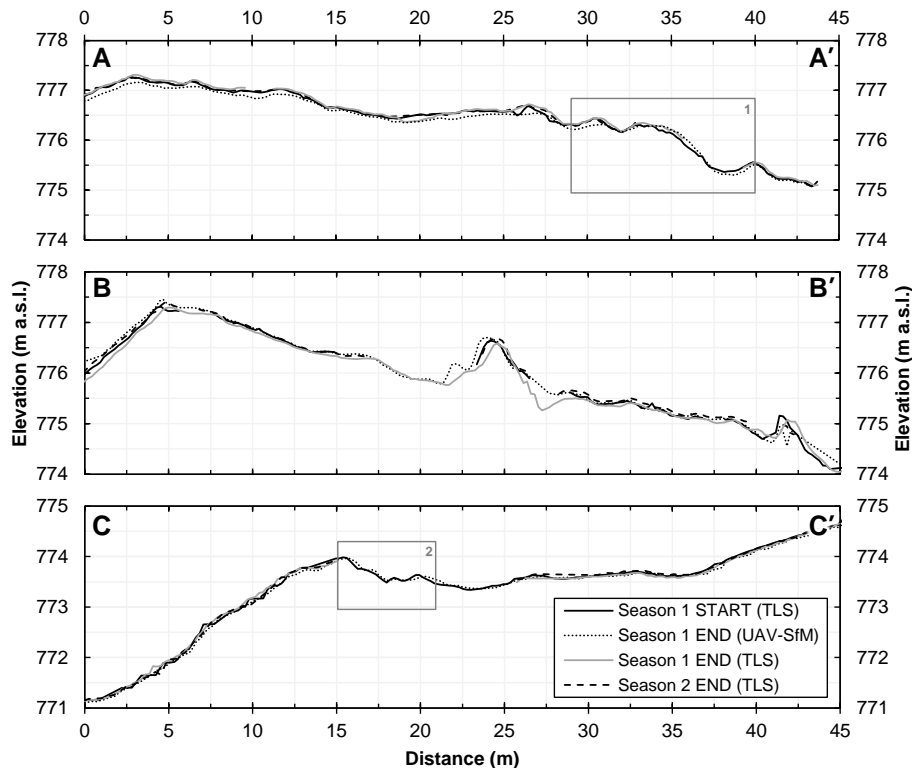


**Figure 5.** Moraine surface elevation profiles, extracted from gridded ( $0.2\text{ m}^2$ ) digital elevation models of TLS- and SfM-derived topographic datasets. Profile locations are shown in Fig. 4. Profiles A and B bisect the main central moraine crest, whilst profile C is located on moraine deposits at the back of the embayment. Inset numbered boxes in profiles A and C show areas referred to in the text.

Title Page

Abstract

Introduction

Conclusions

References

Tables

Figures

◀

▶

◀

▶

Back

Close

Full Screen / Esc

Printer-friendly Version

Interactive Discussion

